

Active motion artifact cancellation for wearable health monitoring sensors using collocated MEMS accelerometers

Peter T. Gibbs, Levi B. Wood, and H. Harry Asada
d'Arbeloff Laboratory for Information Systems and Technology
Department of Mechanical Engineering
Massachusetts Institute of Technology
{ woodl, asada } @mit.edu

ABSTRACT

This paper presents an active noise cancellation technique for recovering wearable biosensor signals corrupted by bodily motion. A finger mounted photoplethysmograph (PPG) ring sensor with a collocated MEMS accelerometer is considered. The system by which finger acceleration disturbs PPG output is identified and a means of modeling this relationship is prescribed using either FIR or Laguerre models. This means of modeling motivates the use of a recursive least squares active noise cancellation technique using the MEMS accelerometer reading as an input for a FIR or Laguerre model. The model parameters are identified and tuned in real time to minimize the power of the recovered PPG signal. Experiments show that the active noise cancellation method can recover pulse information from PPG signals corrupted with up to 2G of acceleration with 85% improvement in mean squared error.

Keywords: Wearable sensors, accelerometer, active noise cancellation, motion artifact reduction, PPG, system ID

1. INTRODUCTION

Wearable medical sensors are expected to be revolutionary in many application areas, ranging from cardiovascular monitoring to battle field personnel monitoring and sports medicine¹. However, wearable sensors are often made unreliable during every day activities leading to corrupted signals and mistaken medical prognosis not found in traditional non-wearable biosensors². Many wearable biosensing systems are meant for use on active, dynamic patients, either in the field or on mobile hospitalized patients. Thus, the sensing systems must be robust with respect to disturbance, especially motion of the wearer. New technology is needed for eliminating motion artifact and recovering signals corrupted by bodily motion.

Accelerometers have long been used for monitoring daily activities of elderly people and rehabilitation patients as well as for clinical monitoring for COPD and others^{3,4}. In this paper, a relationship between body motion and signal corruption will be identified using MEMS accelerometers. Further, a new method for creating a motion tolerant wearable biosensor is demonstrated. A MEMS accelerometer is used with a wearable biosensor not only to monitor the wearer's activities, but also for recovering corrupted biosensor signals using an active noise cancellation algorithm.

In the following, the disturbance dynamics relating the distorted medical sensor signal to the acceleration of the medical sensor will be identified. Using the model structure of the disturbance dynamics an active noise cancellation system will be constructed⁵. Parameters of the disturbance model are estimated such that the recovered signal power may be minimal. A prototype will be developed for a photoplethysmograph (PPG) sensor worn at a finger of the patient. The method will be implemented using a MEMS accelerometer collocated with the PPG sensor. Experiments verified the algorithm.

2. APPROACH

2.1 Motion artifact of photoplethysmograph

Photoplethysmograms (PPG) have become a powerful diagnostic tool for physicians over the last 20 years. In particular, they are capable of providing continuous information regarding a patient's pulse rate, respiratory rate, and oxygen saturation. PPG sensors typically consist of two LEDs and a single photodetector (PD) oriented such that a vascularized region of tissue is encapsulated. Changes in measured light intensity at the photodetector primarily result from changes in the volume of blood in the optical path between the LEDs and PD. As more blood enters the optical path, less light is recorded at the detector.

PPG is appropriate for wearable sensor applications, since it is compact and power efficient. Figure 1 shows a miniaturized PPG sensor attached to a finger: the MIT Ring Sensor⁵. It is capable of detecting a PPG signal at the base of the finger. Figure 2-a shows the anatomy of a finger and the arterial network. Figure 2-b shows the arrangement of LED and PD.

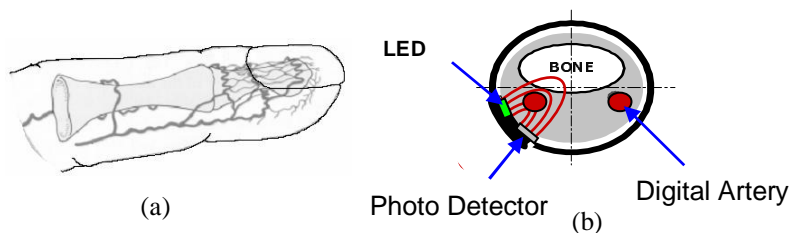


Figure 1: MIT Ring sensor. Figure 2: Anatomy of a digital artery (a) and finger base photoplethysmograph (b).

Despite the salient features, photoplethysmograph sensors are susceptible to motion, often causing false signal due to motion artifact. As illustrated in Figure 2, the blood-filled arterial network is disturbed when exposed to acceleration. The cross-sectional area of the blood vessel may change, and thereby the LED light absorption may be disturbed by the acceleration. Furthermore, the relative location of the digital artery to the LED and PD will change as the sensor body is accelerated. As a result, the PPG sensor output will significantly be disturbed by the finger motion. Although the exact relationship between the finger acceleration and the diameter and location of the blood vessel is unknown, it is clear that the distortion of the PPG waveform is strongly correlated with the acceleration of the finger. Therefore, it will be effective for reducing the PPG distortion if the finger acceleration is measured and is correlated with the signal distortion.

2.2 Active noise cancellation

Active Noise Cancellation is a powerful tool for recovering the desired signal from corrupted ones. It is applicable to a PPG wearable sensor susceptible to motion. The key concept is to measure the patient's motion with a multi-axis MEMS accelerometer incorporated into the sensor body, and use the acceleration information to correct the motion-corrupted signal. The distortion of the PPG signal may be estimated based on adaptive filtering technology. Figure 3 shows the block diagram of active noise cancellation. The ring sensor detects the mixture of the true signal denoted y_o and the distorted signal w , which are assumed to be additive. The actual motion is measured with the MEMS accelerometer. Then the adaptive filter estimates the dynamics of the distortion process, and produces the estimate of the distorted signal \hat{w} caused by the acceleration a . The estimated distortion \hat{w} is then subtracted from the PPG sensor output y . The adaptive filter comprises a disturbance dynamics model predicting how the distorted signal component is generated in response to the body acceleration. The model parameters are estimated in real-time such that the recovered signal may have a minimum variance.

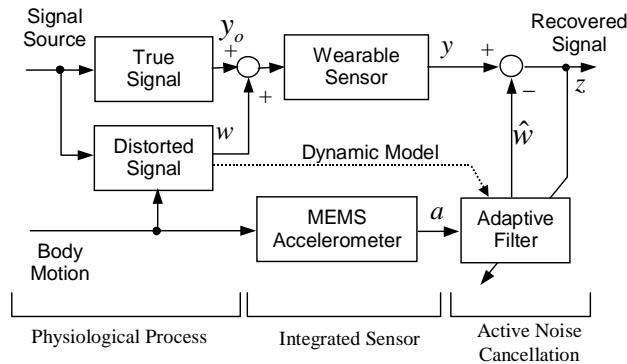


Figure 3: Block diagram of motion tolerant wearable biosensor system with accelerometer and active noise cancellation filter.

3. DISTURBANCE DYNAMICS

3.1 Preliminary experiments on disturbance dynamics

There are a few technical issues in applying the active noise cancellation method to motion artifact reduction for the wearable PPG sensor. First, the model structure of the disturbance dynamics must be known prior to implementation. This entails experimental and theoretical studies as to how the system dynamics relate a distorted PPG signal to the measured acceleration. Second, the disturbance model must be simple enough to estimate in real time. A low-order, compact model is necessary for minimizing the number of parameters to be estimated in real time. Third, the standard active noise cancellation algorithm assumes that disturbance is uncorrelated to the true signal as well as to the distorted signal⁶. This, too, requires both theoretical and experimental considerations for verifying the assumption or modifying the methodology. In this section, the first two issues will be addressed, and the third issue will be discussed in section 4.



Figure 4: Accelerometer and PPG sensor placement on hand and finger.

Preliminary experiments were conducted to investigate the model structure of disturbance dynamics. Figure 4 shows an experimental apparatus consisting of a PPG sensor and a MEMS accelerometer. The PPG signal consists of two components; one is the pulsatile signal due to the cardiac activity, called the cardiac signal, and the other is a distorted signal due to the finger acceleration. The objective of the preliminary experiment is to single out the distorted signal and examine the dynamic relationship with the acceleration. To this end an inflatable cuff is attached to the upper arm of a human subject to temporally shut out the pulsatile component coming from the cardiac activity. Then the finger is shaken to observe the distorted PPG signal in response to the finger acceleration. The experimental procedure is to obtain a good pulse signal from the PPG sensor, then inflate the pressure cuff to 160mmHg whereat the artery collapses and the pulse signal completely flat lines. At this point, the blood volume within the finger is constant and the blood is quiescent. Finally, the finger can be accelerated and the output can be measured, free of the pulsatile signal. The pressure cuff must be inflated quickly and the data taken immediately after cuff inflation so that the capillaries and veins do not have time to significantly change shape as they attempt to supply more oxygen to the tissue. The Massachusetts

Institute of Technology Committee On The Use of Humans as Experimental Subjects (Approval No. 3117) has approved the use of the ring sensor and accelerometer, and has approved the use of pressure cuffs inflated to systolic pressure (160mmHg).

Figure 5 shows one of the preliminary experiments of disturbance dynamics. Note that no pulsatile component due to the cardiac activity is present in the measured PPG signal, and that the PPG signal is strongly correlated to the acceleration. Figure 6 shows the PPG response to an impact applied to the hand. Note that the response of the PPG signal is substantially time delayed from the time of the input (approximately 100-130 ms) as can be seen by comparing the peak times. Figure 7 shows that the FIR model requires the PPG signal to be shifted left by 80ms in order to achieve the best noise cancellation whereas the Laguerre filter obtains the best filter without phase shift. This issue of phase shift with the FIR filter is not present if the filter order is allowed to be long enough to traverse the time delay and then some, but long filters are not computationally feasible. Also noticeable from Fig. 6 is that the PPG response slowly decays after the acceleration has come back to zero. This reveals that the disturbance dynamic has a slow dominant pole.

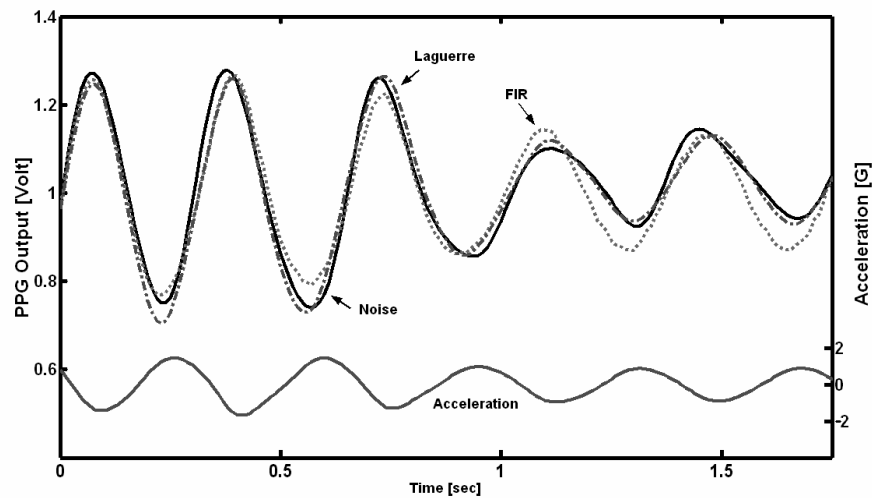


Figure 5: Experimental data, FIR and Laguerre models with model order 15.

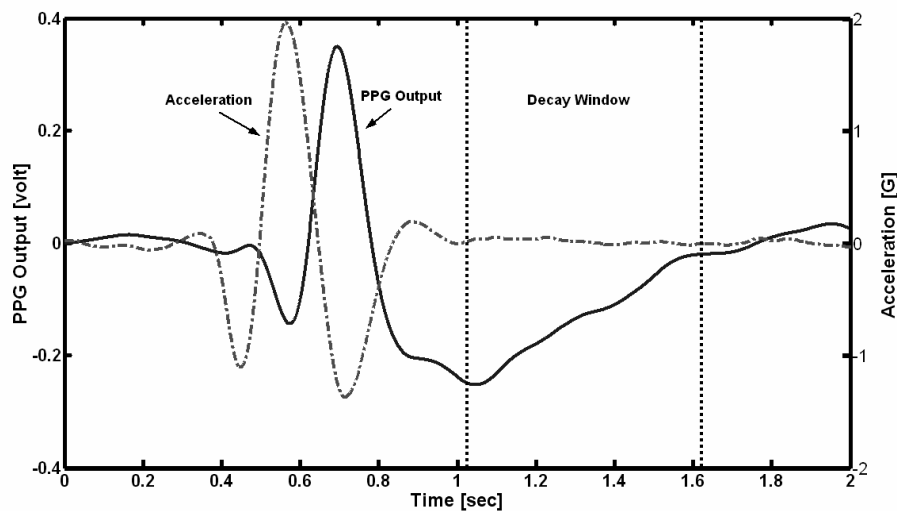


Figure 6: PPG output in response to an impact applied to the hand.

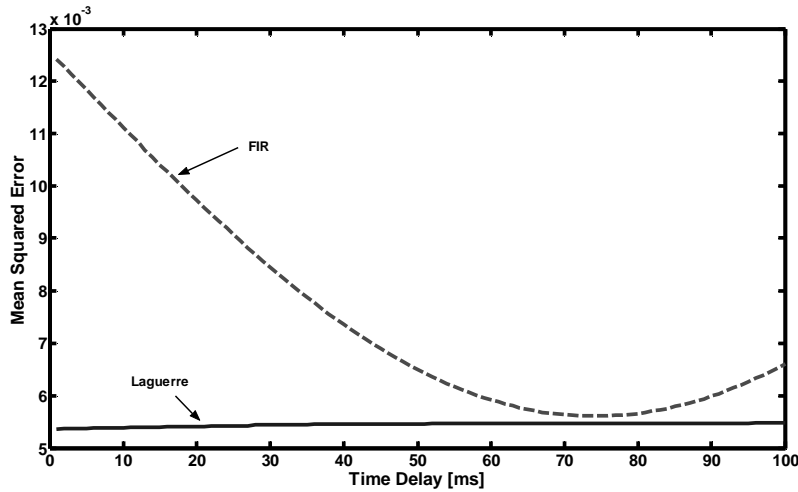


Figure 7: Mean squared error versus time delay for FIR and Laguerre models with order 7 filter.

3.2 Disturbance model order and reduction

Based on disturbance dynamics experimentation, the structure of the disturbance dynamics is determined in this section. For adaptive filter design, a Finite Impulse Response (FIR) model is straightforward and easy to deal with. Therefore, we begin with a FIR model for representing the disturbance dynamics relating the distorted signal, w , to the acceleration, a :

$$w(t) = \varphi(t)^T \theta(t) \quad (1)$$

where

$$\begin{aligned} \varphi(t) &= [a(t-1) \cdots a(t-i) \cdots a(t-n)]^T \\ \theta(t) &= [b_1 \cdots b_i \cdots b_n] \end{aligned}$$

with $a(t)$ being the acceleration measured at each time step and b_i being coefficients to be determined.

The FIR model, although simple and straightforward, needs a large number of parameters, particularly when the response has a slow decaying mode. As shown in Figure 6 above, the disturbance dynamic has a slow mode. An alternative to the standard FIR model is to use a special series of expansion functions, such as the Laguerre series expansion. Instead of utilizing the delay operator as a basis, it could be useful to make use of a Laguerre basis, which utilizes knowledge of the dominant system dynamics to describe the disturbance system. In this way the output can be expressed as

$$w(t) = \sum_{i=1}^n \bar{g}_i L_i(q, \alpha) a(t) \quad (2)$$

where

$$\begin{aligned} L_i(q, \alpha) &= \frac{K}{q - \alpha} \left(\frac{1 - \alpha q}{q - \alpha} \right)^{i-1} \\ K &= \sqrt{1 - \alpha^2} \end{aligned}$$

for which q is the delay operator and $|\alpha| < 1$ is the dominant system pole described in the discrete domain.

In Figure 5, both a FIR model and a Laguerre model are used for approximating the PPG response to acceleration. For the same number of parameters used, the Laguerre model has a significantly smaller error compared to the FIR model. The Laguerre model needs an additional parameter, α , for the expansion functions. Since a true impulse cannot be produced, the closest approximation possible that the human body can attain under its own power is attempted. This prevents the subject under consideration from being damaged by a motion machine. Figure 6 shows the attempted impact.

The dominant discrete pole can be approximated by determining the dominant continuous pole. This can be accomplished by disturbing the system with an impulse and observing the decay time. Then the continuous pole can be determined by using the rule of thumb that decay time equals five times the dominant time constant. This means that

$$\bar{\alpha} = \frac{5}{\text{Decay Time}} \quad (3)$$

where $\bar{\alpha}$ is the continuous pole corresponding to the discrete time pole, α . Finally, the transformation from the real domain to the discrete domain can be implemented to determine the correct discrete pole:

$$\alpha = e^{-\bar{\alpha}T} \quad (4)$$

The decay window shown in Fig. 6 is the time between when the input acceleration stops and when the output PPG levels off. For the ring sensor system, the decay time appears to be approximately 0.6 seconds. Thus, the dominant time constant, continuous and discrete time poles can be determined and are presented in Table I.

Table I: Values leading to the computation of the dominant discrete time pole.

Decay Time	Time Constant	Continuous Pole	Discrete Pole, α
0.6 sec	0.12 sec	8.33/sec	0.92

The above approximation of the dominant discrete time pole, α , is a gross one at best. However Laguerre model construction with α between 0 and 1, incremented by steps of 0.01, shows that the best result is always obtained with α very close to 0.92.

Using the approximated value for the discrete pole, the Laguerre model can now be determined along with the FIR model. Employing the methods described in section 3.3 with a sampling rate of 100Hz and using a model order of 15 for both the FIR and Laguerre models yields Fig. 5.

For both the FIR and Laguerre models, increasing the filter order beyond 15 improves the curve fit, but even with a filter order of 15, both curves match very well, with the Laguerre model fitting better than the FIR model. Sampling rate can also alter the curve fit and the filter order required to achieve a particular level of curve fit. This topic will not be covered here, but preliminary trials have shown that 100Hz is nearly optimal.

It should be noted that the output generated from this experiment may not be entirely indicative of the PPG-acceleration system dynamics when the brachial artery is open and functioning normally. With the artery and veins shut off at the upper arm, the entire arm may act as a bladder with wave reflection. The hope is, however, that this modification to the system dynamics negligibly alters the output.

3.3 Modeling

The parameters required for both the FIR and Laguerre models can be easily determined using the least squares formula

$$\hat{\theta} = PB; \quad P = \left[\sum_{t=1}^l \varphi(t)\varphi(t)^T \right]^{-1}, \quad B = \sum_{t=1}^l w(t)\varphi(t) \quad (5)$$

where $\varphi(t)$ is a moving column vector of discrete time accelerations whose length is the filter order, as previously defined. The vector is a sliding window that traverses the entire acceleration vector. Also, $w(t)$ is the measured PPG output and l is the size of the data set. This will yield a parameter vector $\hat{\theta}$ whose length is the filter order such that the estimated disturbance is

$$\hat{w}(t) = \varphi(t)^T \hat{\theta} \quad (6)$$

The least squares formula is easily adapted to the Laguerre basis transformation discussed in the previous section. The change is that, instead of letting $\varphi(t) = [a(t-1) \cdots a(t-i) \cdots a(t-n)]^T$ as for the FIR case, the input parameters should

become $\varphi(t)=[L_1a(t)\cdots L_i a(t)\cdots L_n a(t)]^T$. The result from the least squared formula will be $\hat{g}=[\hat{g}_1\cdots\hat{g}_i\cdots\hat{g}_n]$ instead of $\hat{\theta}$ for the FIR model.

4. ACTIVE NOISE CANCELLATION

4.1 Active noise cancellation

Based upon the ability to model the disturbance system previously demonstrated, a dynamic, self tuning model predicting the distortion of the PPG ring sensor signal in response to acceleration has been built. Both FIR and Laguerre models will be considered here since the FIR model requires attention to time delay that the Laguerre model does not. The FIR coefficients are estimated in real-time to minimize the variance of the recovered signal.

As shown in Fig. 2 for the additive model case, y_o is the heart portion of the PPG signal and w is the distortion signal component added to the true signal. The actual PPG sensor output y is corrupted and is given by $y = y_o + w$. Let \hat{w} be an estimate of the distorted signal component to be created by the adaptive filter. The objective of the adaptive filter is to minimize the error $w - \hat{w}$. This can be achieved by evaluating the signal power of the recovered signal $z = y - \hat{w}$:

$$E[z^2] = E[(y_o + w - \hat{w})^2] = E[y_o^2] + 2E[y_o w] - 2E[y_o \hat{w}] + E[(w - \hat{w})^2] \quad (7)$$

Note that the true PPG signal y_o that is generated by the heartbeat is assumed to be uncorrelated with the body motion and thereby uncorrelated with the distorted signal component w and its estimate \hat{w} . Therefore, the second and the third terms in the above equation vanish providing that y_o has a zero mean (this requirement will be later discussed). In consequence, minimizing $E[z^2]$ is equivalent to minimizing $E[(w - \hat{w})^2]$, since the first term $E[y_o^2]$ is irrelevant to minimization with respect to the filter coefficients. This is essentially Widrow's Active Noise Cancellation⁶. The above algorithm does not assume prior knowledge of the values of process parameters, but it continuously adjusts the model parameters to minimize the error between y and y_o through minimizing the power in z .

For the purposes of this work, it will be assumed that there is no correlation between bodily motion and heart beat. This may not always be the case, as bodily motion and pulse often tend to synchronize during rhythmic activities⁸. One possible means of dealing with this issue is by shutting off parameter adaptation during times that accelerometer and PPG signals are strongly correlated.

Ensuring that the mean of the desired pulse signal, y_o , is zero is impossible. It is, however, possible to shift the distorted signal, y , such that it has a zero mean. This will satisfy the requirement that y_o must have a zero mean as long as the input acceleration has a zero mean, which would give the distorted portion of the signal, w , a zero mean given the assumption that

$$y = y_o + w \quad (8)$$

The process parameters to identify are the FIR coefficients generating the estimate of distorted signal \hat{w}

$$\hat{w}(t) = \theta(t)^T \cdot \varphi(t) \quad (9)$$

where

$$\begin{aligned} \theta(t) &= [b_1 \cdots b_i \cdots b_n]^T \\ \varphi(t) &= [a(t-d) \cdots a(t-d-i) \cdots a(t-d-n+1)]^T \end{aligned}$$

The regressor $\varphi(t)$ consists of a delayed time sequence of measured acceleration, $a(t-d) \cdots a(t-d-i) \cdots a(t-d-n+1)$. Note that b_i is the i -th FIR parameter and n is the model order, as with the batch processing, and d is the time delay. These parameters are determined in real time to minimize the signal power, z^2 . This parameter estimation can be performed with various real-time computation algorithms, including the standard Recursive Least Squares (RLS), which was implemented in this study.

To apply adaptive noise cancellation with the Laguerre basis, it is necessary to recursively compute the elements of the regressor $\varphi(t)=[L_1a(t)\cdots L_i a(t)\cdots L_n a(t)]^T=[\varphi_1\cdots\varphi_i\cdots\varphi_n]^T$. This can be done by expanding equation (2) to yield

$$\begin{aligned}\varphi_1(t) &= \alpha\varphi_1(t-1) + \sqrt{1-\alpha^2}a(t-1) \\ \varphi_i(t) &= \alpha\varphi_i(t-1) + \varphi_{i-1}(t-1) - \alpha\varphi_{i-1}(t),\end{aligned}\tag{10}$$

which is recursive in both time and i .

The values of d and n are the two most important issues in designing the FIR filter. The model order, n , must be chosen such that the time window considered by the model is large enough to accurately model the system, while at the same time remaining a reasonable order to allow for real time computation. Likewise, the time delay, d , between the input acceleration and the observable response in the system must be determined. It turns out that the time delay that yields optimal results is between 70ms and 110ms for most people. The problem is that some form of a calibration, using both a stationary and excited sensor must be utilized on each person that the ring is to be utilized with. For the purposes of this paper, consideration will only be given to $d=0$ for comparison with Laguerre filtering. For more information on model order, n , and time delay, d see reference 7.

The Laguerre basis transformation is a suitable means for dealing with the time delay issue. Figure 7 shows that the optimal time delay (in the sense of reducing error) with the Laguerre basis is 0. Even while considering a time delay with the FIR model, the Laguerre model without time delay produces a smaller error. Thus the Laguerre model appears to be a suitable model choice.

4.2 Experimental results

An experiment was performed wherein a PPG ring sensor with a collocated MEMS accelerometer was fixed to a pinky finger on the right hand. Also, a second reference PPG sensor was placed on the individual's left pinky finger. The finger with the collocated accelerometer was excited by the individual exciting the arm in the horizontal plane and in the direction of the digital artery. The individual was sitting and both arms were at approximately heart level. Data was taken simultaneously from the accelerometer and the two PPG sensors, sampled at 100Hz.

Figure 7 shows the acceleration and the reference and disturbed PPG with the FIR and Laguerre signal reconstructions. Both reconstructions utilized a filter order of 7 and $\alpha=0.92$ for the Laguerre filter. No time delay was used for either reconstruction.

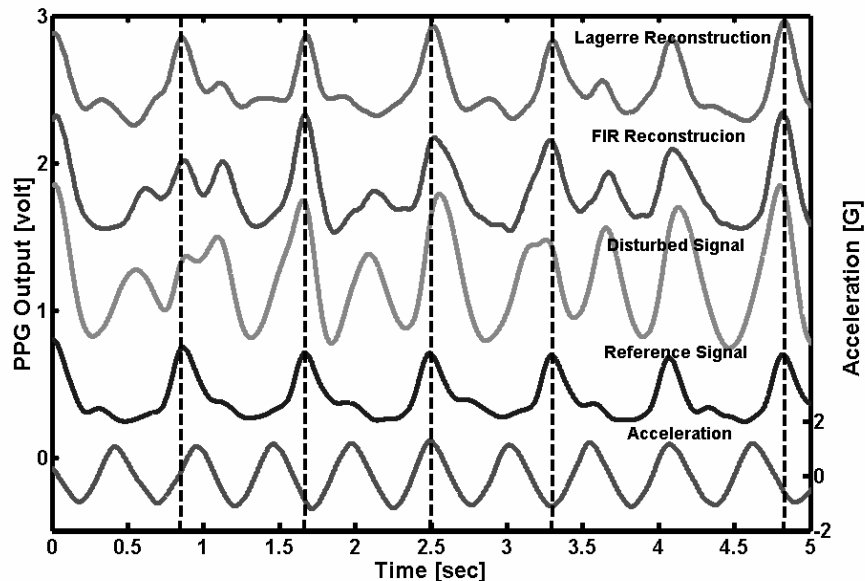


Figure 8: Active Noise cancellation results with FIR and Laguerre filter ($n=7$, sampling rate 100Hz, and $\alpha=0.92$ for Laguerre).

Figure 8 shows that both reconstructions identify every peak of the pulse signal, when compared with the reference signal, whereas the peaks of the corrupted signal do not generally match the reference signal. The average time difference between the peak times of the reference and both reconstructed signals is approximately 10ms. The mean squared error between the reference signal and the disturbed signal is 0.0450 whereas the means squared error between the reference signal and the FIR filtered signal is 0.0134. The error between the reference signal and the Laguerre filtered signal is 0.0063. This represents a 70% reduction of error with the FIR filter and an 85% reduction in error with the Laguerre filter. Also, the overall waveform of the Laguerre corrected signal takes the form of the reference pulse signal whereas the disturbed signal does not resemble the reference signal at all.

5. CONCLUSION

This work has related input acceleration, measured by means of a MEMS accelerometer to blood disturbance measured in the form of a PPG sensor output by means of both FIR and Laguerre models. Further, an active noise cancellation technique, using both FIR and Laguerre disturbance models was implemented. Experiments have shown that the FIR model can accurately recover peak pulse time information with regularity and greatly reduce the mean squared error between the input reference signal and the final output without considering time delay. However, the Laguerre model, also without considering time delay, reduces error by 15% more than the FIR filter and produces a waveform that greatly resembles the reference signal. The filter order is small enough that these methods can be implemented in real time. Thus, acceleration measurement can be used as a means of removing disturbance for wearable biosensors. This system could potentially be improved in the future by development of a first principles model that describes the input acceleration-digital blood volume relationship.

ACKNOWLEDGMENTS

This work is supported by National Institute of Health Grant, No. 1 R21 EB002258-01. The analytic aspect of the work is supported by the National Science Foundation under Grant No. NSF CMS-0330280.

Experimental data and preliminary theory were provided and developed by Hong-Hui Jiang.

REFERENCES

- [1] Asada, H, Shaltis P, Reisner A, Rhee S, Hutchinson RC., "Wearable PPG-BioSensors", IEEE Engineering in Medicine and Biology Magazine, Vol.22, No.3, pp. 28-40, 2003.
- [2] Reisner, A., Shaltis, P., McCombie, D., and Asada, H., "A Critical Appraisal of Opportunities for Wearable Medical Sensors", Proceedings of 2004 IEEE EMBS Conference, 2004.
- [3] Aminian K, Robert P, Buchser EE, Rutschmann B, Hayoz D, Depairon M, "Physical activity monitoring based on acceletrometry: Validation and comparison with video observation", *Med Biol Eng Comput*, 37(3): 304-308, 1999.
- [4] Bussmann, J.B., J.H. Tulen, E.C. van Herel, and H.J. Stam, *Quantification of physical activities by means of ambulatory accelerometry: a validation study*. Psychophysiology, 35(5): p. 488-96, 1998.
- [5] Rhee, S-W., Yang, B-H, and Asada, H., "Artifact-Resistant, Power-Efficient Design of Finger-Ring Plethysmographic Sensors", *IEEE Transactions on Biomedical Engineering*, Vol.48, No.7, pp.795-805, July 2001.
- [6] Bernard Widrow, Robert C. Goodlin et al., "Adaptive Noise Canceling: Principles and Applications", Proceedings of the IEEE, vol. 63, pp. 1692-1716, Dec.1975.
- [7] Jiang, Hong-Hui, Asada, H. Harry, and Gibbs, Peter, "Active Noise Cancellation Using MEMS Accelerometers for Motion-Tolerant Wearable Biosensors", Proceedings of 2004 IEEE EMBS Conference, 2004.
- [8] Niizeki K, Kawahara K, Miyamoto Y, "Cardiac, respiratory, and locomotor coordination during walking in humans", *Folia Primatol (Basel)*. 1996;66(1-4):226-39.